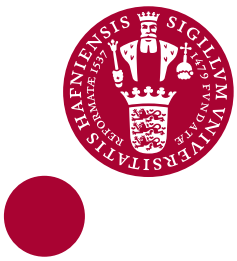

In Situ Monitoring of Nanostructure Formation during the Digestion of Mayonnaise

Salentinig, Stefan; Amenitsch, Heinz; Yaghmur, Anan

Published in:
ACS Omega

DOI:
10.1021/acsomega.7b00153

Publication date:
2017

ACS OMEGA

Article

http://pubs.acs.org/journal/acsodf

In Situ Monitoring of Nanostructure Formation during the Digestion of Mayonnaise

Stefan Salentinig,*[,†] Heinz Amenitsch,[‡] and Anan Yaghmur[§]

[†]Laboratory for Biointerfaces, Department Materials Meet Life, Empa, Swiss Federal Laboratories for Materials Science and Technology, Lerchenfeldstrasse 5, 9014 St. Gallen, Switzerland

[‡]Institute for Inorganic Chemistry, Graz University of Technology, Stremayergasse 9/V, 8010 Graz, Austria

[§]Department of Pharmacy, Faculty of Health and Medical Sciences, University of Copenhagen, Universitetsparken 2, DK-2100 Copenhagen Ø, Denmark

ABSTRACT: Triglycerides in food products such as mayonnaise are a vital source of energy and essential for a complete and healthy diet. Their molecular structures consist of a glycerol backbone esterified with fatty acids on the two outer and the middle positions. During the digestion of triglycerides by pancreatic lipase in the small intestine, the ester bonds on the outer positions are hydrolyzed, leading to amphiphilic monoglycerides and free fatty acids as products. Depending on their chain length and degree of saturation, these products can self-assemble into a variety of structures in excess water. In this study, we report the discovery of highly ordered nanostructures inside of the mayonnaise emulsion droplets during in vitro digestion of mayonnaise under simulated in vivo conditions using time-resolved synchrotron small-angle X-ray scattering. The formation of these structures is most likely linked to their function as a carrier and controlled release system for food nutrients, especially poorly water-soluble components, in the aqueous milieu of the digestive tract. This detailed understanding of nanostructure formation during the digestion of triglyceride-containing food products such as mayonnaise may have fundamental implications for the development of foods with improved nutritional and functional properties.

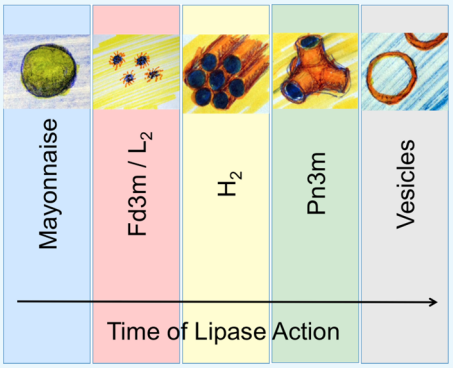

INTRODUCTION

Mayonnaise is an oil-in-water emulsion, consisting of egg-lecithin-stabilized oil droplets that contain up to 80% vegetable oil triglycerides. The latter are mainly composed of unsaturated fatty acids (approximately 90% of the fatty acids).[1−3] The closely packed foam of oil droplets in mayonnaise is a vital source of nutrients and energy. On the molecular level, triglycerides have a glycerol backbone with ester bonds to three fatty acids at the stereochemically distinct positions: sn-1, sn-2, and sn-3. The digestion of the triglycerides by lipases in the human digestive tract converts these water-insoluble molecules to more polar products for their absorption into the circulatory system of the body.[4] Pancreatic lipase in the small intestine quantitatively transfers the triglycerides into amphiphilic sn-2 monoglycerides and two free fatty acids.[5,6] In excess water, these molecules can self-assemble into a variety of structures including highly organized nanostructures that are in thermodynamic equilibrium with the surrounding aqueous medium.[7−10] The structure of these self-assembled systems can be modulated by temperature and lipid composition,[7,11] selected amino acids or peptides,[12,13] pH,[10,14,15] and certain ions[16] and can generally be described by the critical packing parameter.[17]

Complex colloidal systems consisting of highly organized, self-assembled nanostructures inside of the emulsion droplets were found during the digestion of model triolein-based emulsions and milk.[18−21] These complex systems may secure nutrient uptake and act as nanocarriers to deliver poorly water-soluble food components such as polyunsaturated fatty acids under compromised bile salt conditions.[18,21] Similar nanostructures were also discussed as oral delivery vehicles for poorly water-soluble bioactive food components (e.g., carotenes, vitamins A, D, E, and K) or drugs.[13,22−25] The colloidal structures that are formed during the triglyceride digestion were reported to be highly pH responsive: Increasing the pH in the continuous dispersion phase was found to decrease the critical packing parameter because of charge repulsion of deprotonated oleic acid molecules.[10,15,17] In terms of variations in the interface curvature, this corresponds to an increase in the negative curvature of the inverse structures, and eventually significant structural alterations occur at higher pH values. Interestingly, an elevated apparent pK_a of the carboxylic group from ∼4.8 to physiologically relevant values in the small intestine, between 6 and 7, was observed for long-chain unsaturated fatty acids such as oleic acid in these self-assembled systems.[10] Yet, no systematic study of the influence of in situ pH increase at values typically occurring within the digestive tract has been performed during lipolysis of emulsions

Received: February 9, 2017
Accepted: March 31, 2017
Published: April 12, 2017

DOI: 10.1021/acsomega.7b00153
ACS Omega 2017, 2, 1441−1446

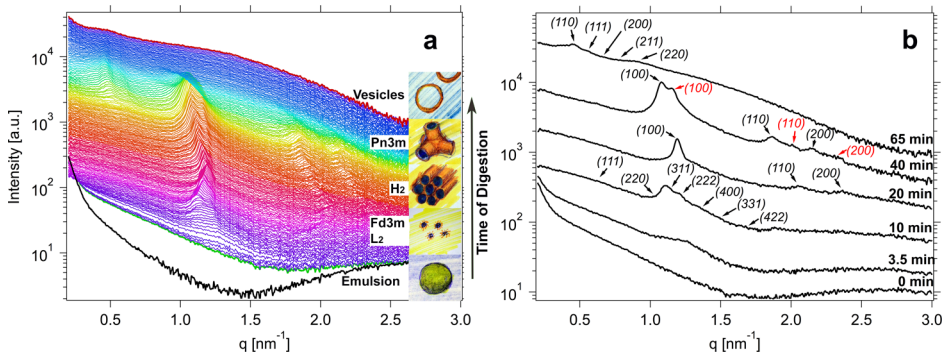

Figure 1. (a) In situ SAXS profiles acquired during the lipolysis of mayonnaise combined with increasing pH from 6.5 to 7.4 over 80 min. The black SAXS profile is given for mayonnaise at pH 6.5 before lipase addition and titration. Upon addition of lipase, the SAXS profiles were recorded every 30 s up to 80 min of lipolysis. The insets present an artistic view of the nanostructural transitions of normal (oil−water) emulsion via inverse micellar phases, H_2 and $Pn\bar{3}m$ to vesicles and sponge phase, in agreement with the SAXS data. (b) Representative SAXS profiles from (a) with identifiable Bragg peaks and further calculated theoretical peak positions indexed with the corresponding Miller indices for the micellar cubic $Fd\bar{3}m$ phase at 10 min; the H_2 phase at 20 and 40 min (second coexisting H_2 indexed in red); and the bicontinuous cubic $Pn\bar{3}m$ phase at 65 min possibly coexisting with vesicles and sponge phase.

containing triglycerides. Hence, in this study, we combine the lipolysis with a pH ramp from ∼6.5 to 7.5 during the digestion of mayonnaise. This simulates the increase in pH of the food bolus as it passes through the small intestine and is also the pH range where lipase has its maximum activity.[26] To our knowledge, this is the first report on real-time monitoring of nanostructures that are generated during the digestion of mayonnaise, using synchrotron small-angle X-ray scattering (SAXS) under selected pH conditions of the small intestine.

Understanding the dynamic colloidal transformations during digestion of complex food systems and the involved alterations in the nanostructural features can provide important information on the role of these nanostructures in the delivery of bioactive food components. The nanostructural features of these systems were further reported to affect the progress of the lipolysis, indicating the potential to use these nanostructures to steer the lipid digestion process.[27] Hence, a detailed understanding of the nanostructure formation in food products such as mayonnaise can open new opportunities for the design of functional foods with a potential of avoiding or even curing food-related health issues such as obesity and vitamin malabsorption and further minimizing the risk of coronary heart disease and cancer.[28−30]

RESULTS AND DISCUSSION

The in situ SAXS data for the digestion of mayonnaise combined with gradual pH increase from pH 6.5 to 7.4 are presented in Figure 1. Before the addition of pancreatin extract, the SAXS pattern shows an oil-in-water emulsion with the low-q upturn in the $I(q)$ from the scattering of the large emulsion particles and protein aggregates in mayonnaise. The broad correlation peak with a maximum around $q \approx 2.8$ nm^{-1} in this curve may result from the local structural organization of the triglycerides.[31,32]

After the addition of pancreatin extract, containing the pancreatic lipase, significant and fast ordering of the molecules within the oil droplets in the emulsion occurred. A broad correlation peak at $q \approx 1.2$ nm^{-1}, most likely attributed to newly generated inverse micelles (L_2 phase) inside of the emulsion droplets, was visible within a digestion time, t, of 30 s. After 2 min of digestion, several reflections characteristic of an intermediate discontinuous cubic $Fd\bar{3}m$ phase were detected, which started to vanish again after 10 min. At $t > 10$ min, three Bragg peaks characteristic of a newly formed inverse hexagonal (H_2) phase started to dominate the SAXS signal. Interestingly, a second coexisting H_2 phase with smaller lattice dimensions appeared between $t \approx 33$ and 53 min. The complex and the dynamic composition of the mayonnaise oil droplets may cause the coexistence of two H_2 phases with different lattice constants during digestion. The kinetics of lipid digestion was shown to depend on the size of the oil droplet and the lengths of the triglyceride chain among other factors.[6,18] This might lead to droplets with different extent of digestion during the lipolysis process, affecting the transfer of hydrophobic and amphiphilic molecules among their internal structural features. The dynamic lipid redistribution regulating the structural properties of coexisting liquid crystalline particles of different composition was reported previously.[37] From $t > 53$ min, the larger H_2 phase coexisted with the inverse bicontinuous cubic $Pn\bar{3}m$ structure up to 63 min of digestion only when the Bragg reflections from the cubic $Pn\bar{3}m$ phase were detectable. The SAXS patterns at $t > 63$ min were dominated by diffuse scattering, indicating the possible generation and coexistence of the cubic phase with vesicles or a sponge phase. This signal may also result from a growing number of interlamellar attachments on the outside of cubosomes, representing a transition state between the liquid crystalline interior phase and the outside of the vesicular structure, as reported previously.[34] At $t > 73$ min, the Bragg reflections characteristic of the cubic $Pn\bar{3}m$ phase were diminished and a broad hump around $q \approx 0.4$ nm^{-1} was detected. This SAXS curve indicates the coexistence of a sponge phase (L_3 phase) with vesicles.[33] Hence, the swelling of the water channels of the bicontinuous cubic phase by the charged lipids further reduces the curvature, resulting in the transition to the sponge phase with significantly larger water pore dimensions, coexisting with flat lamellar phases in the form of vesicles.[33,35,36] This scattering pattern remains almost without any change, suggesting the end of the digestion process after $t \approx 73$ min. These results show that the digestion process triggered a transition from a mayonnaise emulsion droplet to a unique family of micellar and nonlamellar liquid crystalline dispersions, in line with the expectation considering the critical packing parameter in such systems.

To further study the effect of pH on lipolysis, mayonnaise was also digested at constant pH = 7.0 (Figure 2a). After pancreatin addition at this pH, the broad correlation peak

DOI: 10.1021/acsomega.7b00153
ACS Omega 2017, 2, 1441−1446

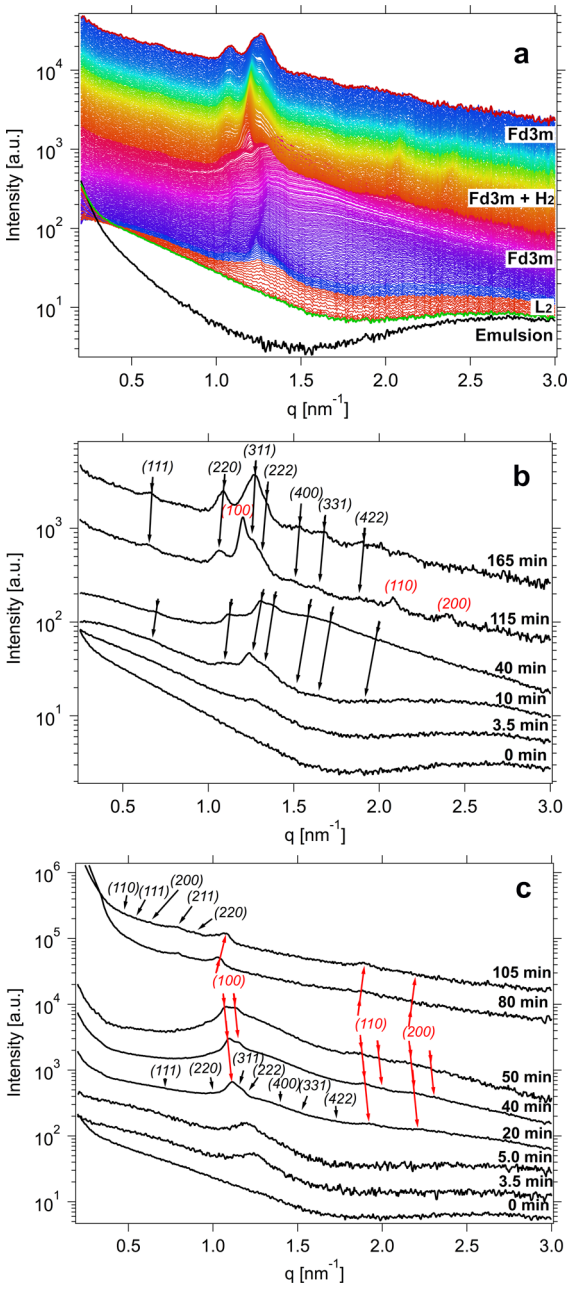

Figure 2. (a) SAXS profiles for the digestion of mayonnaise over 170 min at a constant pH of 7.0. The black SAXS profile is given for mayonnaise before lipase addition. Upon addition of lipase, the SAXS profiles were recorded every 30 s up to 170 min of lipolysis. (b) Representative SAXS profiles from (a) at different time points of digestion. The figure presents the identifiable Bragg peaks and further calculated theoretical peak positions indexed with the corresponding Miller indices for the cubic $Fd\bar{3}m$ between 10 and 165 min in black and the coexisting H_2 phase at 115 min in red. (c) Representative SAXS profiles for the digestion of mayonnaise at constant pH 7.5 over 105 min. The identifiable Bragg peaks and further calculated theoretical peak positions indexed with the corresponding Miller indices for the $Fd\bar{3}m$ at 20 min in black, the biphasic H_2/ H_2 feature between 20 and 105 min in red, and the $Pn\bar{3}m$ at 105 min in black. Further increase in digestion time did not induce significant changes in the obtained SAXS pattern, indicating that the biphasic $Pn\bar{3}m/H_2$ feature was stable and not affected with increasing digestion.

characteristic of intermediate inverse micelles started to appear at $q \approx 1.2$ nm^{-1} during the first 10 min (the early stage of digestion). After $t \approx 10$ min of lipolysis, a structural transition to a neat cubic $Fd\bar{3}m$ phase occurred, and from $t > 60$ min, a coexistence region of the discontinuous cubic $Fd\bar{3}m$ and H_2 phases was detected with the H_2 phase dominating the signal after around 80 min of digestion (Figure 2b). Interestingly, from 80 min onward, the detected Bragg reflections of the $Fd\bar{3}m$ cubic phase started to grow again and dominated the signal from 150 min. No significant changes in the scattering pattern were observed after 150 min, indicating that the lattice constants of coexisting liquid crystalline phases were not affected in the last stage of digestion. Interestingly, compared with the digestion combined with pH increase presented before, the formation of highly ordered nanostructures and structural transitions appear much slower. The dynamic transitions from $Fd\bar{3}m$ to H_2 and then back to $Fd\bar{3}m$ again may result from the exchange of materials between emulsion droplets of different colloidal structures or extent of digestion. Similar transfer phenomena of hydrophobic or amphiphilic molecules between internal self-assembled lipidic particles were previously discussed, and a structural transition from the micellar cubic $Fd\bar{3}m$ phase to emulsified microemulsions via hexosomes was observed on mixing with normal oil emulsions within 60 min.[37]

The structural transitions during mayonnaise digestion at constant pH = 7.5, presented in Figure 2c, also confirm the transition from normal emulsion to highly ordered nanostructures. In the first stage of the digestion process, at $t \approx 3$ min, a broad correlation peak indicating the formation of inverse micelles was detected, followed by the Bragg reflections characteristic of inverse cubic $Fd\bar{3}m$ and H_2 phases after $t \approx 7$ min of digestion. The biphasic H_2/H_2 region was observed from around 15 min followed by $H_2/Pn\bar{3}m$ coexistence region at the end of digestion (after $t \approx 85$ min) when no further changes in scattering could be observed.

The changes in lattice constant, a, over the time of mayonnaise lipolysis, calculated from the SAXS patterns under the different pH conditions, are summarized in Figure 3. Upon increasing pH during lipolysis, the lattice constant of the $Fd\bar{3}m$ structure increases from ~16.5 to 17.5 nm between 2 and 10 min of lipolysis. For the following H_2 structure between $t \approx 10$ and 53 min of digestion, a increased from 6.2 to 7.4 nm (see Figure 3a). Interestingly, a second coexisting H_2 phase appeared between 33 and 53 min with around 0.5 nm smaller lattice dimensions. The lattice dimensions of the cubic $Pn\bar{3}m$ phase, dominating the SAXS pattern between 53 and 73 min, gradually increased from 24.2 to 27.9 nm.

For the digestion at constant pH 7.0, presented in Figure 3b, the lattice constant of the $Fd\bar{3}m$ phase decreased from ~16.7 to 16.0 nm within the first 40 min of digestion, followed by a gradual increase to ~16.5 nm at 100 min, and remained constant up to 180 min, whereas the lattice constant of the H_2 phase decreased from ~6.2 to 6.0 nm between 60 and 100 min of digestion and remained relatively constant up to ~150 min when the H_2 reflections diminished again.

The lattice constant of the $Fd\bar{3}m$ phase between 5 and 10 min of lipolysis at pH 7.5 decreased from 17.0 to 15.7 nm (see Figure 3c). The lattice constant of the coexisting H_2 structure increased from ~6.2 to 6.7 nm, with a coexisting bicontinuous cubic $Pn\bar{3}m$ phase from 65 min until the end of the digestion process at 105 min.

These results show that the colloidal transitions from normal oil emulsion to highly ordered nanostructures were faster at elevated pH: The H_2 phase occurred already after ~7 min of

DOI: 10.1021/acsomega.7b00153
ACS Omega 2017, 2, 1441−1446

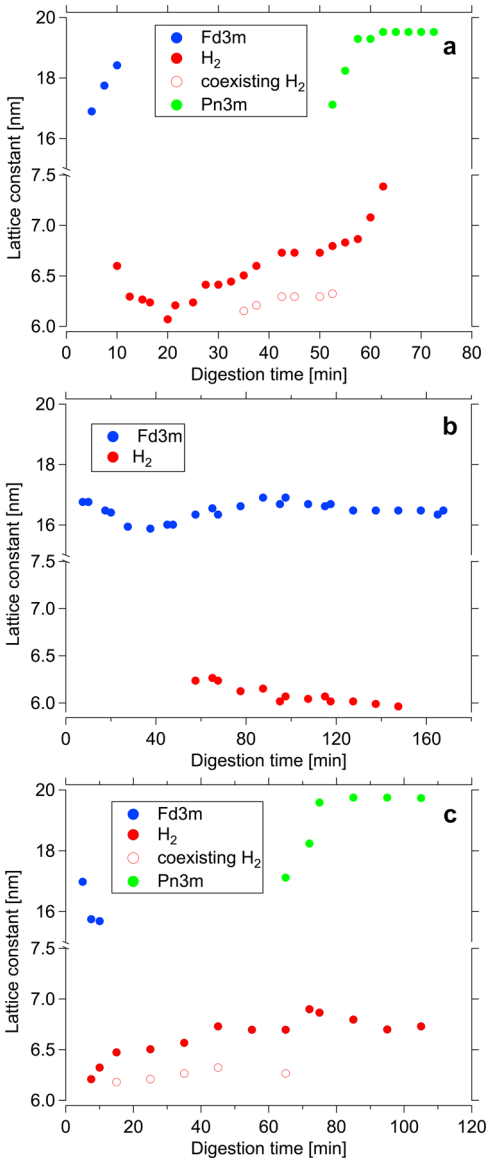

Figure 3. Calculated lattice constants of the detected nonlamellar liquid crystalline nanostructures during lipolysis of mayonnaise combined with increasing pH from 6.5 to 7.4 over 80 min (a) and the experiments at constant pH 7.0 (b) and 7.5 (c). The lattice constants of these phases were calculated from the SAXS profiles presented in Figures 1 and 2.

digestion at pH 7.5 compared with 60 min at pH 7.0. It is interesting that the lattice dimensions of this H_2 phase were also strongly dependent on pH conditions. Whereas the lattice dimensions increased gradually from ∼6.2 to 7.4 nm during the lipolysis coupled with pH increase from 6.5 to 7.4, it decreased from ∼6.2 to 6.0 nm at constant pH 7.0 and increased from ∼6.2 to 6.9 nm at constant pH 7.5. The deprotonation of fatty acids at elevated pH > 6.5, the apparent pK_a of long-chain fatty acids observed in self-assembled structures, could further increase the surface charge density.[10] The resultant charge repulsion between the negatively charged carboxylic groups at the oil−water interface could have a significant impact on the packing geometry and the detected nanostructural features. Hence, the higher pH value toward the end of the small intestine supports colloidal transformations from hydrophobic to more hydrophilic structures. Steric and electrostatic interactions between the digestion products at the oil−water interface are thought to be responsible for these structural transitions.

The pH-dependent fatty acid−water interfacial film of the emulsion droplets might be responsible for the modified digestion kinetics observed in this study and therefore could also affect the detected sequence of phase transitions during the digestion of mayonnaise. Deprotonated fatty acids at pH 7.0 and 7.5 together with monoglycerides can cover the oil−water interface, which could also inhibit the lipase accessibility to their less surface-active triglyceride substrates. This inhibition of lipolysis has been recently discussed as a self-regulatory process of digestion with monoglycerides.[38−40]

The difference in the structural features at the end of the digestion experiments has direct implications on the exchange of materials with the surrounding aqueous phase: The colloidal transformation from emulsion droplets via nonlamellar structures to vesicles may induce the release of encapsulated bioactive food components from the internal lipidic structure to the surface of the vesicle bilayer and the surrounding continuous aqueous medium. In contrast to the internal oil−water interface in nonlamellar structures, the vesicle bilayer is in direct contact with the surrounding medium and allows their interaction with the enterocytes in the digestive tract. The similarity in bilayer curvature among the newly formed vesicles at the end of digestion and the basic mosaic bilayer structure of cell membranes may further promote their interaction.[24] This can then increase the absorption of the lipolysis products and solubilized bioactive components into the circulatory system of the body. Compared with molecular transport, colloids also enhance the number of fatty acid and monoglyceride molecules available for uptake by the enterocytes.[41] Fatty acids and monoglycerides then enter the enterocytes as monomers.

In general, the sequence of the colloidal transformations observed during mayonnaise digestion is in agreement with our previous reports on triolein emulsions and milk at constant pH 6.5.[18,21] In contrast to the digestion of milk, no equidistant characteristic peaks indicating the formation of multilamellar structures such as onion-type vesicles or bilayer stacks were observed during mayonnaise digestion. This is most likely attributed to a difference in the lipid type and composition in mayonnaise as compared to milk. Milk contains a significant amount of saturated fatty acids that may be responsible for the occurrence of coexisting multilamellar vesicular structures. In addition, these colloidal particulate systems are different in the concentration and type of their proteins and bioactive components.

SUMMARY AND CONCLUSIONS

The interfacial active main products from lipolysis of mayonnaise, monoglycerides and free fatty acids, transformed the oil inside of the mayonnaise emulsion droplets to more hydrophilic, highly organized self-assembled structures with a substantial internal oil−water surface area: The oil-in-water emulsion was converted to emulsified microemulsions, micellar cubic $Fd\bar{3}m$ phase, inverse H_2 phase, $Pn\bar{3}m$-type cubosomes, and finally sponge (L_3) phase and vesicles when the pH was increased from 6.5 to 7.4 during the digestion process. These self-assembled nanostructures agreed well with the anticipated behavior based on the critical packing parameter for the amphiphilic molecules that are generated during the mayonnaise digestion process. Time of digestion and pH strongly influence the nanostructural features and transformations. At

DOI: 10.1021/acsomega.7b00153
ACS Omega 2017, 2, 1441−1446

constant pH, the nanostructure formation and structural transitions appeared slower compared with those at continuous pH increase. Hence, an increase in pH during lipolysis seems to further promote the transformation of the hydrophobic oil environment inside of the mayonnaise emulsion droplet to highly organized hydrophilic interfaces and vesicles as final structures. The highly ordered nanostructures, found during the mayonnaise digestion under simulated in vivo conditions, dominate the phase behavior in this study. Hence, the generation of these nano-self-assemblies may provide a plausible mechanistic pathway for in vivo lipid digestion under high triglyceride content or compromised bile salt conditions. These dynamic structures and their transformations may then maintain the digestion process and have direct implications on the transport and delivery of hydrophobic bioactive food components such as carotenoids, hydrophobic vitamins, or drugs.

MATERIALS AND METHODS

Materials. Pancreatin from porcine pancreas (8× USP grade pancreatin activity) was purchased from Sigma-Aldrich (St. Louis, MO, USA). It is a mixture of digestive enzymes produced by the exocrine cells of the porcine pancreas and contains enzymes such as lipase, amylase, trypsin, ribonuclease, and protease. NaOH (0.2 M) and HCl (0.2 M) (p.a. grade, Sigma-Aldrich, St. Louis, MO, USA) were used for pH adjustment. Mayonnaise was store-bought, having 71.5% fat content with 8.0% saturated fatty acids, 1.6% carbohydrates, 1.3% proteins, and 1% salt. Mayonnaise (1 mL) was dissolved in 9 mL of 40 mM phosphate-buffered saline (PBS) buffer at the relevant pH for the digestion experiment (6.5, 7.0, and 7.5). Ultrapure water (R > 18 MΩ) was used for the preparation of all samples.

Methods. *Flow through Lipolysis Model.* In vitro digestion was conducted in a thermostated glass vessel at 37 °C under constant magnetic stirring. For pH control and adjustment, a pH electrode (Microelectrode, Metrohm AG, Switzerland) was interlocked via a computer with a pump (model 540060, TSE Systems GmbH., Germany) loaded with a 5 mL syringe containing 0.2 M NaOH. A custom-build computer program triggered the pH-controlled release of the NaOH from the syringe pump into the reaction vessel to maintain or increase the pH of the simulated digestive juice during the digestion in the reaction vessel.

Mayonnaise (1 mL) was added to 40 mM PBS buffer (9 mL) in the reaction vessel, before the addition of pancreatin extract. The digestion medium was continuously drawn from the reaction vessel through a 1.5 mm diameter quartz capillary mounted in the X-ray beam and back into the vessel at a flow rate of approximately 10 mL/min to avoid beam damage, through silicone tubing (total volume ∼1.5 mL) via a peristaltic pump. SAXS patterns were recorded for 27 s with a 3 s delay between frames. The digestion reaction was then initiated by the addition of 1 mL of pancreatin from porcine pancreas solution (0.1 g in 1 mL of 40 mM PBS buffer) within ∼1 s using a second remotely operated syringe pump (model PHD 4400, Harvard Apparatus, MA, US) installed at the beamline.

Small-Angle X-ray Scattering. In vitro digestion SAXS measurements were recorded at the Austrian SAXS beamline at Elettra (Trieste, Italy).[43] An X-ray beam having a wavelength of 1.54 Å was used, with a sample to detector distance of 1314 mm providing a q-range of $0.07 < q < 4.5$ nm^{-1} where q is the length of the scattering vector, defined by $q = 4\pi/\lambda \sin(\theta/2)$, λ is the wavelength, and θ is the scattering angle. The 2D SAXS patterns were acquired for 27 s with 3 s delay between frames, using a PILATUS3 1M detector (Dectris Ltd., Baden, Switzerland; active area of 169 × 179 mm^2 with a pixel size of 172 μm). The 2D SAXS patterns were integrated into one-dimensional scattering function $I(q)$ using FIT2D[42] and then analyzed using IGOR pro (WaveMetrics, Inc., Lake Oswego, OR). Hexagonal, cubic, and lamellar liquid crystalline space groups were determined, indexing the relative positions of the Bragg peaks in the scattering profiles.[7] Microemulsions and unilamellar vesicles were characterized using their unique scattering signatures (e.g., the broad correlation peak reflecting the mean particle-to-particle distance for micelles and the q^{-2} dependence at low q values for locally flat bilayer structures). Further information on the SAXS data analysis can be found elsewhere.[18]

AUTHOR INFORMATION

Corresponding Author

*E-mail: stefan.salentinig@gmail.com, stefan.salentinig@empa.ch (S.S.).

ORCID

Stefan Salentinig: 0000-0002-7541-2734

Anan Yaghmur: 0000-0003-1608-773X

Notes

The authors declare no competing financial interest.

ACKNOWLEDGMENTS

The scattering studies in this article were conducted at the Austrian SAXS beamline (Elettra synchrotron station, Trieste, Italy). S.S. acknowledges the funding from the SNSF (grant number 200021_169513).

REFERENCES

(1) Eastwood, G.; Watson, P.; Bierenbaum, M. L.; Fleischman, A. I. Fatty Acids and Other Lipids in Mayonnaise. *J. Am. Diet. Assoc.* **1963**, *42*, 518−520.

(2) Depree, J. A.; Savage, G. P. Physical and Flavour Stability of Mayonnaise. *Trends Food Sci. Technol.* **2001**, *12*, 157−163.

(3) Jacobsen, C.; Schwarz, K.; Stöckmann, H.; Meyer, A. S.; Adler-Nissen, J. Partitioning of Selected Antioxidants in Mayonnaise. *J. Agric. Food Chem.* **1999**, *47*, 3601−3610.

(4) Carey, M. C.; Small, D. M.; Bliss, C. M. Lipid Digestion and Absorption. *Annu. Rev. Physiol.* **1983**, *45*, 651−677.

(5) Borgström, B. Influence of Bile Salt, pH, and Time on the Action of Pancreatic Lipase; Physiological Implications. *J. Lipid Res.* **1964**, *5*, 522−531.

(6) Salentinig, S.; Yepuri, N. R.; Hawley, A.; Boyd, B. J.; Gilbert, E.; Darwish, T. A. Selective Deuteration for Molecular Insights into the Digestion of Medium Chain Triglycerides. *Chem. Phys. Lipids* **2015**, *190*, 43−50.

(7) Yaghmur, A.; de Campo, L.; Sagalowicz, L.; Leser, M. E.; Glatter, O. Emulsified Microemulsions and Oil-Containing Liquid Crystalline Phases. *Langmuir* **2005**, *21*, 569−577.

(8) de Campo, L.; Yaghmur, A.; Sagalowicz, L.; Leser, M. E.; Watzke, H.; Glatter, O. Reversible Phase Transitions in Emulsified Nano-structured Lipid Systems. *Langmuir* **2004**, *20*, 5254−5261.

(9) Nakano, M.; Teshigawara, T.; Sugita, A.; Leesajakul, W.; Taniguchi, A.; Kamo, T.; Matsuoka, H.; Handa, T. Dispersions of Liquid Crystalline Phases of the Monoolein/Oleic Acid/Pluronic F127 System. *Langmuir* **2002**, *18*, 9283−9288.

(10) Salentinig, S.; Sagalowicz, L.; Glatter, O. Self-Assembled Structures and pK_a Value of Oleic Acid in Systems of Biological Relevance. *Langmuir* **2010**, *26*, 11670−11679.

DOI: 10.1021/acsomega.7b00153
ACS Omega 2017, 2, 1441−1446

(11) Caboi, F.; Amico, G. S.; Pitzalis, P.; Monduzzi, M.; Nylander, T.; Larsson, K. Addition of Hydrophilic and Lipophilic Compounds of Biological Relevance to the Monoolein/Water System. I. Phase Behavior. *Chem. Phys. Lipids* **2001**, *109*, 47−62.
(12) Chemelli, A.; Conde-Valentín, B.; Uhlig, F.; Glatter, O. Amino Acid Induced Modification of Self-Assembled Monoglyceride-Based Nanostructures. *Langmuir* **2015**, *31*, 10377−10381.
(13) Gontsarik, M.; Buhmann, M. T.; Yaghmur, A.; Ren, Q.; Maniura-Weber, K.; Salentinig, S. Antimicrobial Peptide-Driven Colloidal Transformations in Liquid-Crystalline Nanocarriers. *J. Phys. Chem. Lett.* **2016**, *7*, 3482−3486.
(14) Negrini, R.; Mezzenga, R. pH-Responsive Lyotropic Liquid Crystals for Controlled Drug Delivery. *Langmuir* **2011**, *27*, 5296−5303.
(15) Salentinig, S.; Phan, S.; Darwish, T. A.; Kirby, N.; Boyd, B. J.; Gilbert, E. P. pH-Responsive Micelles Based on Caprylic Acid. *Langmuir* **2014**, *30*, 7296−7303.
(16) Yaghmur, A.; Laggner, P.; Sartori, B.; Rappolt, M. Calcium Triggered Lα-H_2 Phase Transition Monitored by Combined Rapid Mixing and Time-Resolved Synchrotron SAXS. *PLoS One* **2008**, *3*, No. e2072.
(17) Israelachvili, J. N. *Intermolecular and Surface Forces*, 3rd ed.; Academic Press: Sydney, 2011; pp 535−569.
(18) Salentinig, S.; Sagalowicz, L.; Leser, M. E.; Tedeschi, C.; Glatter, O. Transitions in the Internal Structure of Lipid Droplets During Fat Digestion. *Soft Matter* **2011**, *7*, 650−661.
(19) Marze, S.; Gaillard, C.; Roblin, P. In Vitro Digestion of Emulsions: High Spatiotemporal Resolution Using Synchrotron SAXS. *Soft Matter* **2015**, *11*, 5365−5373.
(20) Patton, J. S.; Carey, M. C. Watching Fat Digestion. *Science* **1979**, *204*, 145−148.
(21) Salentinig, S.; Phan, S.; Hawley, A.; Boyd, B. J. Self-Assembly Structure Formation During the Digestion of Human Breast Milk. *Angew. Chem., Int. Ed.* **2015**, *54*, 1600−1603.
(22) Sagalowicz, L.; Leser, M. E. Delivery Systems for Liquid Food Products. *Curr. Opin. Colloid Interface Sci.* **2010**, *15*, 61−72.
(23) Martiel, I.; Sagalowicz, L.; Mezzenga, R. Phospholipid-Based Nonlamellar Mesophases for Delivery Systems: Bridging the Gap between Empirical and Rational Design. *Adv. Colloid Interface Sci.* **2014**, *209*, 127−143.
(24) Porter, C. J. H.; Trevaskis, N. L.; Charman, W. N. Lipids and Lipid-Based Formulations: Optimizing the Oral Delivery of Lipophilic Drugs. *Nat. Rev. Drug Discovery* **2007**, *6*, 231−248.
(25) Sagalowicz, L.; Leser, M. E.; Watzke, H. J.; Michel, M. Monoglyceride Self-Assembly Structures as Delivery Vehicles. *Trends Food Sci. Technol.* **2006**, *17*, 204−214.
(26) Fallingborg, J. Intraluminal Ph of the Human Gastrointestinal Tract. *Dan. Med. Bull.* **1999**, *46*, 183−196.
(27) Barauskas, J.; Anderberg, H.; Svendsen, A.; Nylander, T. Thermomyces Lanuginosus Lipase-Catalyzed Hydrolysis of the Lipid Cubic Liquid Crystalline Nanoparticles. *Colloids Surf., B* **2016**, *137*, 50−59.
(28) Austin, M. A. Plasma Triglyceride and Coronary Heart Disease. *Arterioscler. Thromb.* **1991**, *11*, 2−14.
(29) Unger, R. H.; Zhou, Y. T. Lipotoxicity of Beta-Cells in Obesity and in Other Causes of Fatty Acid Spillover. *Diabetes* **2001**, *50*, S118−S121.
(30) Katan, M. B. Trans Fatty Acids and Plasma Lipoproteins. *Nutr. Rev.* **2009**, *58*, 188−191.
(31) Xenakis, A.; Papadimitriou, V.; Sotiroudis, T. G. Colloidal Structures in Natural Oils. *Curr. Opin. Colloid Interface Sci.* **2010**, *15*, 55−60.
(32) Papadimitriou, V.; Dulle, M.; Wachter, W.; Sotiroudis, T.; Glatter, O.; Xenakis, A. Structure and Dynamics of Veiled Virgin Olive Oil: Influence of Production Conditions and Relation to Its Antioxidant Capacity. *Food Biophys.* **2013**, *8*, 112−121.
(33) Angelov, B.; Angelova, A.; Mutafchieva, R.; Lesieur, S.; Vainio, U.; Garamus, V. M.; Jensen, G. V.; Pedersen, J. S. SAXS Investigation of a Cubic to a Sponge (L_3) Phase Transition in Self-Assembled Lipid Nanocarriers. *Phys. Chem. Chem. Phys.* **2011**, *13*, 3073−3081.
(34) Demurtas, D.; Guichard, P.; Martiel, I.; Mezzenga, R.; Hébert, C.; Sagalowicz, L. Direct Visualization of Dispersed Lipid Bicontinuous Cubic Phases by Cryo-Electron Tomography. *Nat. Commun.* **2015**, *6*, 8915.
(35) Ridell, A.; Ekelund, K.; Evertsson, H.; Engström, S. On the Water Content of the Solvent/Monoolein/Water Sponge (L_3) Phase. *Colloids Surf., A* **2003**, *228*, 17−24.
(36) Engström, S.; Alfons, K.; Rasmusson, M.; Ljusberg-Wahren, H. Solvent-Induced Sponge (L_3) Phases in the Solvent−Monoolein−Water System. In *The Colloid Science of Lipids: New Paradigms for Self-Assembly in Science and Technology*; Lindman, B., Ninham, B. W., Eds.; Steinkopff: Darmstadt, 1998; pp 93−98.
(37) Moitzi, C.; Guillot, S.; Fritz, G.; Salentinig, S.; Glatter, O. Phase Reorganization in Self-Assembled Systems through Interparticle Material Transfer. *Adv. Mater.* **2007**, *19*, 1352−1358.
(38) Reis, P.; Miller, R.; Leser, M.; Watzke, H.; Fainerman, V. B.; Holmberg, K. Adsorption of Polar Lipids at the Water−Oil Interface. *Langmuir* **2008**, *24*, 5781−5786.
(39) Reis, P.; Holmberg, K.; Miller, R.; Krägel, J.; Grigoriev, D. O.; Leser, M. E.; Watzke, H. J. Competition between Lipases and Monoglycerides at Interfaces. *Langmuir* **2008**, *24*, 7400−7407.
(40) Reis, P.; Watzke, H.; Leser, M.; Holmberg, K.; Miller, R. Interfacial Mechanism of Lipolysis as Self-Regulated Process. *Biophys. Chem.* **2010**, *147*, 93−103.
(41) Narayanan, V. S.; Storch, J. Fatty Acid Transfer in Taurodeoxycholate Mixed Micelles. *Biochemistry* **1996**, *35*, 7466−7473.
(42) Hammersley, A.; Thompson, A.; Svensson, S.; Brown, K.; Claustre, L.; Freund, A.; Gonzalez, A.; McSweeney, S.; Moy, J. *Esrf Internal Report*. ESRF98HA01T, FIT2D, 1997; Vol. *9*, pp 129.
(43) Amenitsch, H.; Rappolt, M.; Kriechbaum, M.; Mio, H.; Laggner, P.; Bernstorff, S. First Performance Assessment of the Small-Angle X-ray Scattering Beamline at ELETTRA. *J. Synchrotron Radiat.* **1998**, *5*, 506−508.

DOI: 10.1021/acsomega.7b00153
ACS Omega 2017, 2, 1441−1446